Radiation heat loss and solid combustion products characterisation of premixed Al-air flames

P. Laboureur[1,2], C. Chauveau[1], R. Lomba[3], C. Dumand[2], F. Halter[1,4]
[1] : *ICARE – CNRS, 1C Avenue de la Recherche Scientifique 45071 Orléans, France*
[2] : *PSA Groupe, 1 Route de Gisy 78943 Vélizy-Villacoublay, France*
[3] : *AVL LMM SAS, 5-9 Rue Benoît Frachon 91127 Palaiseau, France*
[4] : *Université d'Orléans*

1 Introduction

Through an increasing global energy consumption based mainly on the use of fossil carbon products, the scientific community agrees that human activity is partly responsible for climate change and global warming. A process of decarbonizing our energies is necessary, however, despite existing clean energy conversion systems, our current incapacity to massively store energy is the main obstacle to the development of these alternative solutions to fossil fuels and pushes to study new energy carriers.

The metallic energy vector can be a solution to answer this challenge, in which metal powders are used to store and convey the energy. Indeed, metal combustion is highly exothermic and oxides formed by this reaction can be recycled using processes powered by renewable energies. The energy carrier would thus be used in a closed loop without generating greenhouse gases over its entire cycle [1].

Aluminum seems to be a potential candidate as a metallic energy vector with interesting energy properties (specific energy 31 MJ/kg), a quantity of raw material sufficient to meet global needs and the existence of a clean zero-carbon recycling industry of these oxides. In contrast, fundamental properties and structures of these Al-air two-phase flames are still poorly known compared to traditional hydrocarbon flames, with differences noted in the literature [2]. However, in order to study the valorization possibilities of the energy released by an Al-air flame and therefore the viability of an energy carrier based on aluminum powders, it is essential to describe properly the combustion process of aluminum particles burning in a dispersed condition. From an energetic overview, it is also essential to evaluate the energy distribution between the radiation, convection and the energy remaining in the condensed phase.

2 Experimental setup

The experimental apparatus consists of a Bunsen type burner with an exit diameter of 32 mm, generating conical premixed metal flames in open field. By Venturi effect, air flow controlled by a digital flowmeter sucks metal particles and generates an aerosol in the burner main body. This one has a particular geometry of expansion and convergence to give to the flow a top-hat velocity profile at the burner exit. A schematic of the experimental apparatus used is shown in [2] and the optical configuration is illustrated in Fig. 1.

Correspondence to: pascal.laboureur@cnrs-orleans.fr

Table 1: Granulometric distribution data of aluminum powders at the burner exit

Characteristic diameter of the particle size distribution	In number	In volume
d_{10} (µm)	0.92	1.77
d_{50} (µm)	2.63	7.58
d_{90} (µm)	4.32	29.38

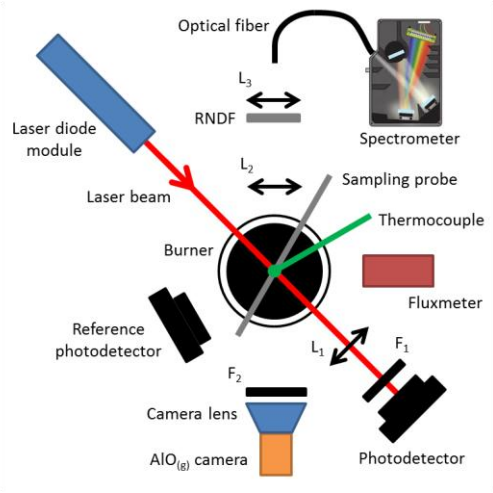

Figure 1: Optical configuration. F_x: band-pass filters, RNDF: reflective neutral density filter, L_x: plano-convex lenses

The aluminum powder used for this study is supplied by Poudres Hermillion. This powder was analyzed by scanning electron microscopy (SEM) coupled with an energy dispersion X-ray spectroscopy (EDS). Aluminum particles are mainly spherical with 98.1% in mass of aluminum and 1.9% in mass of alumina. In order to obtain a more accurate information of the particles size reaching the flame front, the size distribution of particles was measured by Fraunhofer diffraction using a HELOS Sympatec laser diffraction sensor (manufacturer optical module R5, f = 500 mm, laser beam diameter 13 mm, laser power 5 mW, measured diameter range 0.5 - 875 µm) mounted at the burner exit during tests without combustion. Granulometric data are presented in Tab. 1 and are in agreement with images made by SEM of initial powders, showing that there is no particles agglomeration between the tank and the burner exit.

In order to measure in real time the equivalent ratio of the flow, which is an important parameter in the characterization of flame properties, a set consisting of a laser diode module (LDM670 Thorlabs, center wavelength 670 nm, laser power 5.5 mW, beam size 3.2 mm × 3.4 mm), two biased Si photodetectors (DET10A2 Thorlabs, DET100A2 Thorlabs), a plano-convex lens (f_{L1} = 75.8 mm) and a band-pass filter (F_1, center wavelength 671 nm, FWHM 10 nm) is installed on the test bench. The laser beam passes through the flow at the burner center and at 2 mm height, between the burner outlet and the flame base. It is then focused to be measured by the DET100A2 sensor (wavelength range 320 - 1100 nm, active area 75.4 mm²) equipped with the F_1 filter. The concentration is thus estimated by laser attenuation using the Beer-Lambert method :

$$\log\left(\frac{I_0}{I}\right) = \frac{3\, Q_{ext}\, \chi\, B}{2\, \rho\, d}$$

Where I_0 is the beam incident intensity, I is the intensity transmitted by the aerosol, χ is the thickness of the environment traversed, d is the particles diameter, ρ is the mean particles density, B is the concentration at the burner exit and Q_{ext} is the extinction coefficient. Q_{ext} was determined experimentally during tests without combustion using a digital scale to estimate the mass flow rate of dispersed powder and PIV data to measure the flow rate at the burner outlet [2]. A DET10A2 reference sensor (wavelength range 200 - 1100 nm, active area 0.8 mm²) allows subtracting the light emission generated by the flame on the F_1 filter bandwidth.

The combustion is monitored by direct visualization thanks to a camera (AVT MAKO G-419B, acquisition frequency 10 Hz, spatial resolution 20.9 px/mm, exposure time 10 µs) with a camera lens and a band-pass filter (F_2, center wavelength 488 nm, FWHM 6 nm) in front of the camera, highlighting the spatial distribution of $AlO_{(g)}$ reaction intermediate and allowing reconstituting the metal flame structure. In addition, an optical set composed of two plano-convex lenses (f_{L2} = 125 mm, f_{L3} = 53 mm), a UV reflective neutral density filter (optical density 2, spectral range 200 - 1200 nm), an optical fiber of 200 µm in diameter

and a spectrometer (OceanOptics HR4000, wavelength range 200 - 1100 nm, exposure time 10 ms), allows a local spectral detection of the flame and a determination of the temperature of $AlO_{(g)}$ reaction intermediate.

The radiation study of the flame / plume is carried out with a tangential gradient fluxmeter having a viewing angle of 150° and operating for wavelengths between 0.3 and 20 µm. This differential sensor measures only the radiated power flux-density by subtracting the convective flux from the total flux received by the sensor. This calibrated sensor was tested with radiative hydrocarbon diffusion flames.

Finally, solid combustion products are sampled at different heights in the plume and a type K thermocouple provides the average temperature in the sampling zone. These samples are then analyzed by SEM and EDS in order to obtain more precise information on how aluminum particles burn in the flame by examining the shape, size, chemical composition of oxidized particles and studying the presence of residual unburnt.

3 Results and discussions

3.1 Aluminum particles combustion

The overall combustion cycle of an aluminum particle is complex and decomposes into an ignition phase and a chemical reaction phase. Chemical reactions begin once the passive oxidation layer breaks under the effect of thermomechanical stresses, linked to alumina phase changes starting at 900 K [3] and dilatation forces, allowing the free aluminum to react with the oxidizing environment. The oxidation phase of an aluminum particle can be carried out according to three combustion modes [4], as a function of the competition between the reaction kinetics and the diffusion process defined by the Damköhler number (Da).

When the particle diameter is sufficiently large (i.e. for Da >> 1), the combustion takes place in a vapor phase. The liquid aluminum droplet possesses an alumina liquid lobe on its surface due to the initial passive layer covering the particle. A concentric micro-flame is detached from the droplet surface, with a constant flame diameter / droplet diameter ratio around 3.6 for an isolated particle in air [5]. For this combustion regime in air at 1 atm, the adiabatic micro-flame temperature is around 3540 K [6] with the presence of species such as vaporized aluminum and aluminum gaseous sub-oxides which form nanometric oxidized particles in the micro-flame. When the particle diameter is sufficiently small (i.e. for Da << 1), the combustion is controlled by the kinetics and takes place at the particle surface with a combustion temperature not exceeding the aluminum vaporization temperature of 2790 K at 1 atm [4], forming an oxidized particle of similar size to the initial particle and with the presence of aluminum nitrides and aluminum oxynitrides at its surface for temperature below 2550 K [7]. The last mode of aluminum particle combustion consists of a transition mode, which is a combination of the diffusion combustion mode and the kinetic controlled mode. For isolated particles smaller than 10 µm burning in air at 1 atm, simulations have shown that a diffusion flame cannot be self-sustaining except through the additional heat release from heterogeneous surface reactions [8]. Thus, the combustion temperature is close but higher than the aluminum vaporization temperature and the combustion products are a mixture of nanometric and micrometric particles [4].

The combustion products were collected in the plume at 90 mm and for an Al-air flame presenting an equivalence ratio between 0.9 and 1. Under these conditions, the plume temperature at the collection point is 1600 K, the flame is conical with a reaction zone presented in Fig. 3(Left) and the flame top not exceeding a height around 40 mm above the burner exit. The collected particles are composed mainly of nanometric spherical particles smaller than 200 nm in diameter and agglomerated with each other. Among the combustion products, micrometric spherical particles with a diameter ranging from 2.5 µm to 7.5 µm are isolated and mixed into nanometric particles. A SEM image example of collected particles is given in Fig. 2. This picture was selected to illustrate the presence of a spherical particle (5.5 µm in diameter) in the middle of the nanometric particles environment. This particle exhibits a darker zone at its center. Thanks to an EDS probe, the mass chemical composition of combustion products can be estimated. Nanometric

particles are composed of 49.1% aluminum, 44.6% oxygen and 6.3% nitrogen in mass while micrometric particles are composed of 47% oxygen, 46.1% aluminum and 6.9% nitrogen in mass.

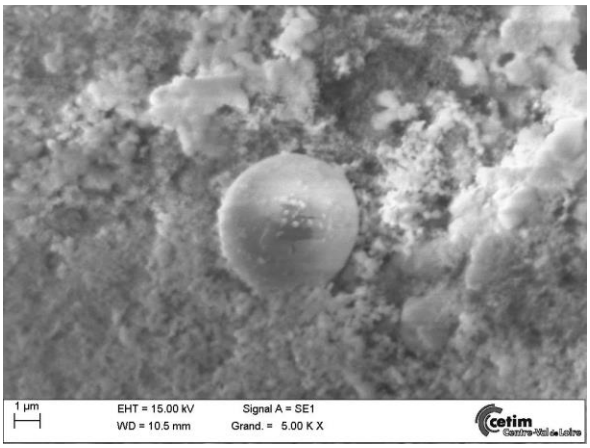

Figure 2: SEM image example of collected particles at 90 mm height and for an Al-air equivalence ratio between 0.9 and 1

As indicated in Tab. 1, in the initial aluminum powder, 50% of the particles are smaller than 2.63 µm in diameter and only 0.67% of the particles have a diameter greater than 9 µm in number. Thus, based on isolated particle studies, the vast majority of initial particles should react in a heterogeneous regime and the expected combustion products should be composed mainly of micrometric spherical particles with a size of the initial particles order. The aluminum mass content obtained by EDS probe indicates that the injected aluminum is fully oxidized. The perfect sphericity of the micrometric particles indicates that they are formed in the liquid state, therefore at high temperature and during the combustion process. According to their number, their size and their composition, it is possible to conclude that these micrometric particles correspond to the alumina lobes residues of larger particles during a vapor phase combustion. The material volume of micrometric combustion products is in agreement with the initial alumina volume of the passive layer covering larger aluminum particles. Although initial particles are rather small, the entirety of particles therefore undergoes a combustion in a diffusion mode and mainly produces nanometric particles. Heating provided by the neighboring particles may promote this combustion mode. This has already been reported for the dust combustion of slightly larger aluminum particles [9].

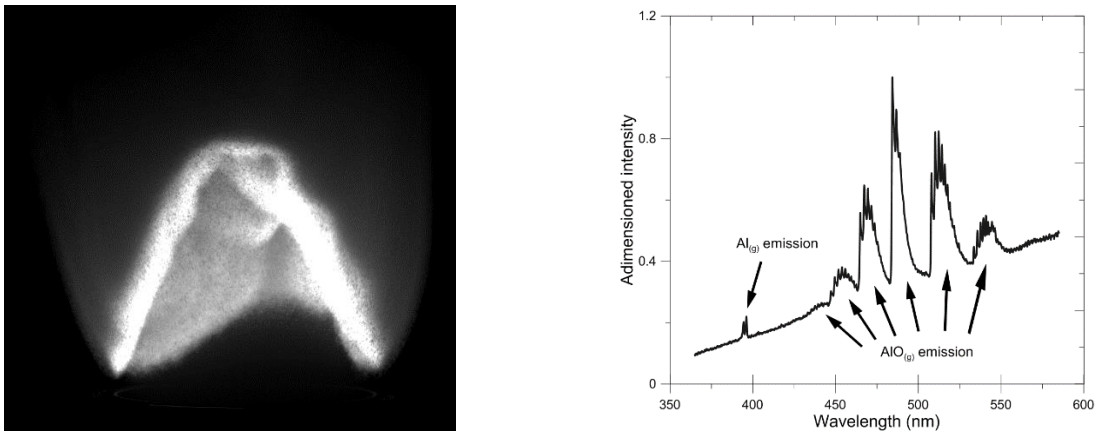

Figure 3. Left: Illustration of the reaction zone through the AlO(g) emission for an Al-air equivalence ratio of 0.95; Right: Example of an adimensioned real emission spectrum of Al-air flame for an equivalence ratio of 0.95

Following the methodology described in Lomba et al. [2], an adimensioned emission spectrum obtained for an Al-air flame with an equivalence ratio of 0.95 is illustrated in Fig. 3 (Right). It is composed of both a continuous background emission due to the thermal radiation of the condensed phase and the gaseous species emission from rotational-vibrational transitions of electronic levels. Concerning gaseous contributions, the $AlO_{(g)}$ emission in the $B^2\Sigma^+ \rightarrow X^2\Sigma^+$ (blue-green) band system is predominant and 396 nm

are also observed. In our experimental setup, the $AlO_{(g)}$ temperature determined by $AlO_{(g)}$ spectral emissions is constant at 3150 K for an Al-air equivalence ratio ranging from 0.64 to 1.39 [2].

Considering a homogeneous distribution at the burner exit and a fixed Al-air equivalence ratio, a mean inter-particle distance can be determined thanks to the Wigner-Seitz radius for a mean diameter of 2.63 µm (see Tab. 1). Thus, the center-to-center mean inter-particle distance is between 126 µm and 97 µm for an Al-air equivalence ratio ranging respectively from 0.64 to 1.39. Keeping the constant ratio of flame diameter / droplet diameter at 3.6, an interaction between two micro-flames should occur for neighboring aluminum particles with a diameter greater than 27 µm, which is unlikely. With our particles density, each particle burns like an isolated particle but with different boundary conditions, explaining that these relatively small particles undergo a combustion mode in diffusion. The temperature estimated by the $AlO_{(g)}$ emission spectrum is consequently only the average reaction temperature of each micro-flame. It does not correspond to the average temperature of the entire gaseous phase, that is the macroscopic flame temperature, and explains that the $AlO_{(g)}$ temperature does not vary according to the global equivalence ratio.

The darker zone on the micrometric particle surface in Fig. 2 seems to be a solid phase composed of aluminum nitride and oxynitrides, which is in agreement with the nitrogen detection by EDS probe. This difference in mass content of elements measured by EDS probe between nanometric reaction products and micrometric particles could be explained by a different phenomenology and a changing reaction mechanism, even if the main species seems to be alumina in both cases. The significant nitrogen content found in the different combustion products indicates that aluminum nitride and oxynitrides production should also be considered in the chemical reactions. Since the creation of aluminum nitride compounds is less sensible enthalphy than the alumina formation, the specific energy of aluminum powders is overvalued.

3.2 Radiation of the aluminum cloud flame

The flame radiation is measured axially for different positions using a fluxmeter. The radial coordinate of the fluxmeter is kept constant for all axial positions at 135 mm from the burner center. The setup being axisymmetric, the method for determining the total radiated power is the same as for traditional burner flames [10] and consists in integrating the axial profile over a cylindrical surface. An axial profile of the radiated power flux-density for an Al-air equivalence ratio of 0.9 is illustrated in Fig. 4. The maximum of the radiated power flux-density is obtained around the flame half-height. The dissymmetry observed in the profile is due to the thermal radiation generated by the condensed combustion products in the plume.

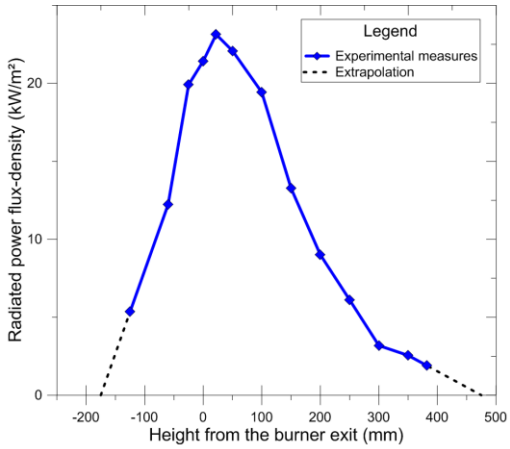

Figure 4: Axial profile of the radiated power flux-density for an Al-air equivalence ratio of 0.9

The vertical profile over a cylindrical surface provides a form factor close to unity. The power outwardly radiated by the flame and the plume can be measured precisely with this method and does not require any assumption on the particles emissivity. For an Al-air equivalence ratio of 0.9, the power radiated by the flame and the plume is of 5.2 kW ± 0.5 kW. As the SEM and EDS analyzes did not reveal any unburnt, the combustion efficiency can be assumed to unity. Considering that the total aluminum quantity injected at the burner exit is oxidized into alumina, the total power released by an Al-air mixture with this equivalence ratio is of 7.6 kW. In these conditions, the radiated part is evaluated at 69% ± 7%. However, if we account of the significant nitrogen content found in the combustion products, the total released power would decrease and

so the radiated part would increase. In comparison, it has been shown that the radiated part of a single magnesium particle combustion is around 40 % [11].

4 Conclusion

The current experimental device enables the stabilization of Aluminum/air premixed flames using micrometric particles, with controlled equivalence ratios ranging from 0.65 to 1.4. With the imposed particles densities, each individual particle crossing the reaction zone (i.e. the conical flame surface) burns like an isolated particle. All particles, even the smallest ones, seem to be oxidized in a diffusion mode since nanometric combustion products are mainly smaller than 200 nm in diameter are produced. Only some micrometric spherical alumina particles were identified in the combustion products and supposed to be issued from the passive alumina covering the largest aluminum particles. The temperature evaluated with $AlO_{(g)}$ emissions does not seem to be representative of the average gaseous phase temperature but rather to the reaction temperature of micro-flames surrounding each particle. From an energetic point of view, the radiation contribution of the flame and the plume to the global heat release was evaluated at about 69% for an equivalence ratio of 0.9. However, this contribution is certainly underestimated because of the detection of aluminum nitride and oxynitrides in the combustion products, formed through less exothermic reactions.

References

[1] Julien P, Bergthorson JM. (2017). Enabling the metal fuel economy: green recycling of metal fuels. Sustain. Energy. Fuels. 1: 615.

[2] Lomba R, Laboureur P, Dumand C, Chauveau C, Halter F. (2018). Determination of aluminum-air burning velocities using PIV and Laser sheet tomography. Proc. Combust. Inst.

[3] Trunov MA, Schoenitz M, Dreizin EL. (2006).Effect of polymorphic phase transformations in alumina layer on ignition of aluminum particles. Combust. Theor. Model. 10: 603.

[4] Bazyn T, Krier H, Glumac N. (2007). Evidence for the transition from the diffusion-limit in aluminum particle combustion. Proc. Combust. Inst. 31: 2021.

[5] Braconnier A, Chauveau C, Halter F, Gallier S. (2018). Detailed analysis of combustion process of a single aluminum particle in air using an improved experimental approach. Int. J. of Energetic Mater. Chem. Propul. 17: 111.

[6] McBride BJ, Gordon S. (1996). Computer Program for Calculation of Complex Chemical Equilibrium and Application II. Nationa Aeronautics and Space Administration. Office of Management. Scientific and Technical Information Program.

[7] Bucher P, Yetter RA, Dryer FL, Parr TP, Hanson-Parr DM, Viceni EP. (1996). Flame structure measurement of single, isolated aluminum particles burning in air. Proc. Combust. Inst. 26: 1899.

[8] Bojko BT, DesJardin PE, Washburn EB. (2014). On modeling the diffusion to kinetically controlled burning limit of micro-sized aluminum particles. Combust.Flame. 161: 3211.

[9] Soo M, Goroshin S, Glumac, Kumashiro K, Vickery J, Frost DL, Bergthorson JM. (2017). Emission and laser absorption spectroscopy of flat flames in aluminum suspensions. Combust.Flame. 230: 238.

[10] Bergman NA, Chakraborty S. (2013). Accidental fires and radiation heat transfer: Investigating the effects of flame impingement on structures. The Journal of Purdue Undergraduate Research. 3: 4.

[11] Shoshin YL, Altman IS. (2002). Integral radiation energy loss during single Mg particle combustion. Combust Sci Technol. 209: 219.